NAZARBAYEV UNIVERSITY

ROLE OF MITOCHONDRIA IN RESPONSE TO ATO/D-VC TREATMENT IN KRAS MUTANT CANCER CELLS

BY

ASKAR MAZHIKENOV

A THESIS SUBMITTED IN PARTIAL FULFILLMENT OF THE REQUIREMENT OF NAZARBAYEV UNIVERSITY FOR THE DEGREE OF MASTER OF SCIENCE IN BIOLOGICAL SCIENCES AND TECHNOLOGIES

APRIL 2024

Student:	Askar Mazhikenov	12/04/2024
Supervisor:	Dos Sarbassov	12/04/2024

Examiners

The M.Sc. thesis of Askar Mazhikenov has been approved by the examiners.

Professor Timo Burster (School of Sciences and Humanities, Nazarbayev University),

Assistant Professor Larisa Lezina (School of Medicine, Nazarbayev University)

Abstract

Kirsten rat sarcoma (KRAS) is a prevalent oncogene which is associated with pancreatic, colorectal and lung cancers. KRAS is frequently mutated in variety of tumors and is linked to poor prognosis around the world. According to growing body of literature, one of main features of KRAS mutated cancer cells is a dysregulated glucose metabolism and continuously activated signaling pathways. Therefore, it became an attractive target to investigate cancer proliferation and adaptation response to various treatment strategies. One of such targeted therapies is recently proposed combination of arsenic trioxide (ATO) and D isoform of Vitamin C (D-VC). It inflicts potent synergistic effect on cancer cells by inducing significant cytotoxic stress ultimately leading to cell death. It was found that this novel ATO and D-VC combined treatment induces apoptosis in the mouse KRAS pancreatic adenocarcinoma cells by stimulating the suicidal mitochondrial reactive oxygen species (ROS) production. One potential target site of this treatment are mitochondria. It is unknown, whether similar response can be achieved in KRAS mutant cancer cells depleted of mitochondria. In this study, we aimed to investigate the role of mitochondria in cells as a pivotal player in response to ATO/D-VC treatment.

Role of mitochondria in response to ATO/D-VC treatment in KRAS mutant cancer cells

Askar Mazhikenov

Table of Contents

List of Figures

(48kDa) bands showing dynamic reduction of proteins. B – normalized levels of UQCRC2 to the loading control (GAPDH). Images were taken and quantified with Odyssey CLx Imaging System (LI-COR).

Figure 10. Evaluation of AK192 and AK(-mito) cell numbers and cell size with Multisizer Coulter Counter 4e (B43905, Beckman Coulter, Life Sciences) just before the ATO/D-VC treatment. (AK192 cell count mean – 492820, AK(-mito) cell count mean – 491020; AK192 cell size mean – 18.41 um, AK(-mito) cell count mean – 18.11 um; error bars indicate standard deviation).

Figure 11. Annexin – PI double staining of AK192 and AK(-mito) cells treated or not with ATO/D-VC. A – distribution of population of cells for annexin and PI status (error bars indicate standard deviation). B – single cell distribution of samples (30 000 events for every condition). C – normalized percentage of alive (AV(-), PI(-)) AK192 and AK(-mito) cells treated with the drug (unpaired, two-tailed t-test; mean of AK192 – 30.17%, mean of AK(-mito) – 56.42%; error bars indicate standard deviation).

Abbreviations

ATP	Adenosine triphosphate
KRAS	Kirsten rat sarcoma
EGF	Epidermal growth factor
mTOR	mammalian Target of Rapamycin
FBS	Fetal bovine serum
GSH	glutathione
ATO	Arsenic trioxide
VC	Vitamin C
CCCP	Carbonyl cyanide m-chlorophenyl hydrazone
PINK1	PTEN-induced putative kinase 1
SDS-PAGE	Sodium dodecyl sulfate-polyacrylamide gel electrophoresis
RIPA	Radioimmuno-precipitation Assay
UQCRC2.	Cytochrome b-c1 complex subunit 2

Acknowledgments

First and foremost, I extend my appreciation to Professor Dos Sarbassov, my supervisor, whose support has been pivotal throughout this remarkable journey. His guidance nurtured my scientific thinking and provided me with invaluable opportunities to delve into the realms of molecular oncology and biochemistry. I am profoundly grateful for the wealth of experience gained under his mentorship, which I am confident will pave the way for my future endeavors.

I am also deeply indebted to the entire team at the Cell Growth and Regulation laboratory. Dr. Agata Burska, our esteemed post-doctoral fellow, and our dedicated PhD students—Aruzhan Dildabek, Nargiz Rakhimgerey, Zhansaya Kanketayeva, Daurenbek Kairatuly, and Bayansulu Ilyassova—have been instrumental in introducing me to experimental methodologies and providing invaluable guidance throughout.

Lastly, but by no means least, I extend my thanks to my family and friends whose unwavering support has been my pillar of strength throughout my academic journey.

Declaration

I declare that the research contained in this thesis, unless otherwise formally indicated within the text, is my original work. The thesis has been written by me its entirety. I duly acknowledged all sources of information which have been used in the thesis. The thesis has not been previously submitted to this or any other university for a degree and does not incorporate any material already submitted for a degree.

Signature  Date: 12.04.2024

1. Introduction

1.1 KRAS is key player of signaling cascade and powerful oncogenic driver.

In the 1980s, Kirsten rat sarcoma (KRAS) gene was discovered from viral genome and described as a prospective oncogene (Tsuchida et al., 1982). When the extracellular growth factor binds to its specific receptor, RAS protein is recruited to the cell membrane and activated. RAS proteins are a family of small G-protein groups, which after its activation leads to conformational change and interaction with various proteins (Colicelli et al., 2004). Activation of the small G-proteins is tightly regulated with guanine exchange factors (GEFs) and GTPase activating factors (GAPs) by phosphorylation of GDP and dephosphorylation of GTP (Zenonos et al., 2013). Two essential signaling pathways mediate cell proliferation and growth are mitogen-activated protein kinases (MAPK) and mammalian target of rapamycin (mTOR) pathways also regulated by the RAS (Zenonos et al., 2013) (Figure 1). Both pathways are activated by binding of ligand to it's specific receptor like epidermal growth factor (EGF) to it's tyrosine kinase receptor (EGFR) and further dimerization and cross phosphorylation (Lemmon et al., 2010). Cell proliferation is under the control of RAF/MEK/ERK pathway: after the activation and dimerization of EGFR, it recruits a protein son of sevenless (SOS) which is GEF and activates RAS by binding GTP (Zenonos et al., 2013). Active and dimeric RAS then phosphorylates MEK1/2 further phosphorylating ERK1/2 (Roberts et al., 2007) and finally activating transcription factor ELK1 which is activator of transcription of genes responsible for cell proliferation (Janknecht et al., 1993). Another pathway which acts through cellular growth upregulation is PI3K-AKT-mTOR pathway. In this pathway, EGFR recruits and activates phosphatidylinositol 3-kinase (PI3K), this enzyme phosphorylates PIP2 to PIP3, then PIP3 activates protein kinase B (AKT/PKB) through phosphoinositide-dependent kinase-1 (PDK) (Porta et al., 2014). The active AKT/PKB can inactivate pro-apoptotic factors and increase resistance to the cell death (Chen et al., 2001). Finally, AKT/PKB activates mTORC1 and mTORC2 which act as major drivers of cell growth by provoking anabolism in the cell (Battaglioni et al., 2022).

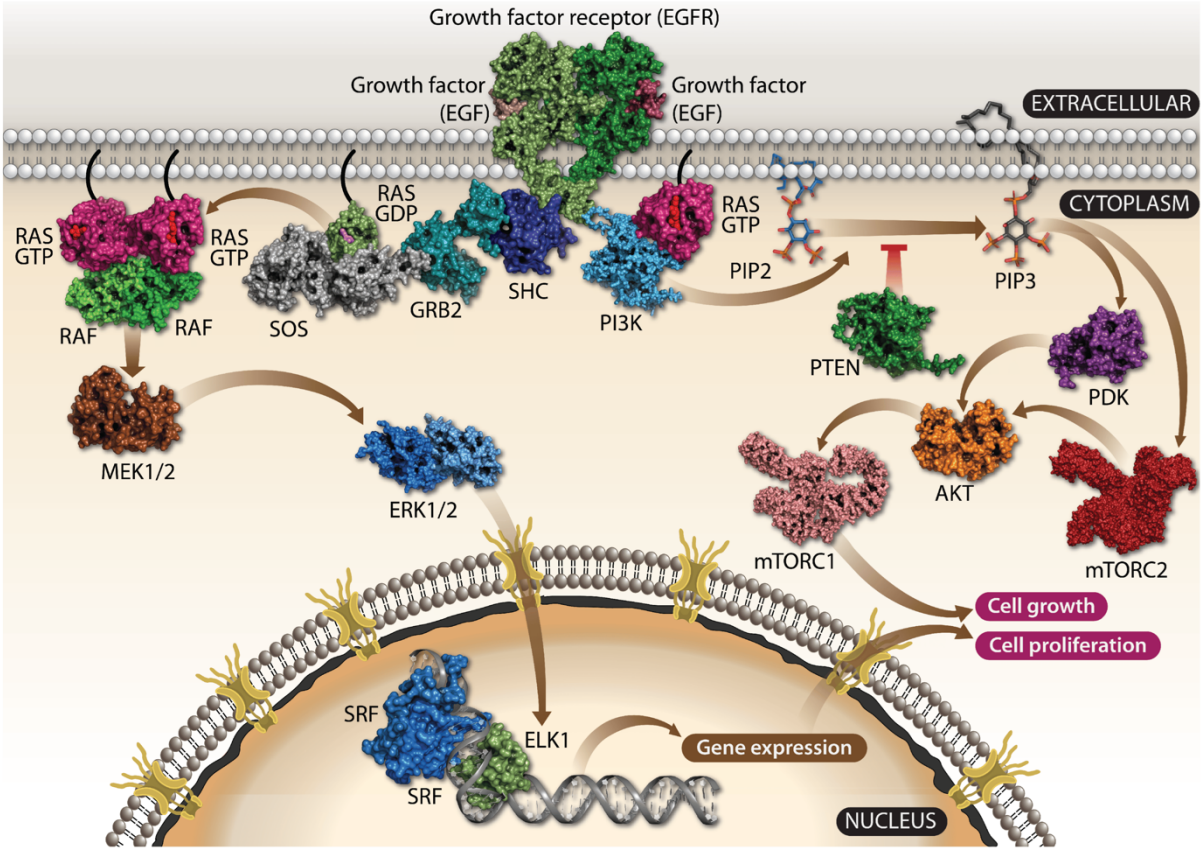

Figure 1. The RAF-MEK-ERK and PI3K-AKT-mTOR pathways are essential RAS effector pathways. RAS signaling, crucial for various cellular processes like proliferation, apoptosis, and growth, represents the archetypal kinase signaling pathway. It initiates with the interaction between a growth factor like EGF and its receptor, a membrane-bound receptor tyrosine kinase (Burska et al., 2022).

Predominant evidence in the literature suggests that mutations in RAS gene indicated in around 25% of all cancer types (Russo et al., 2014). Moreover, specifically KRAS was named as the oncogene “Everest”, since it was shown to appear in 20% of all cancer types and common for malignancies with high mortality. The most frequent mutations which occurs in KRAS gene are G12 and G13 missense mutations. Among the G12 mutation in KRAS, regularly mutated are G12D, G12V, and G12C codon changes - 42%, 28%, and 14% respectively (Pantsar et al., 2018). In previous decades, before Shokat and colleagues discovered obscured pocket, effective treatments for KRAS cancers were lacking (Ostrem et al., 2013), as they were deemed "undruggable" due to KRAS lacking hydrophobic pockets for inhibition (Wang et al., 2013). However, recent progress had led to the development of several KRAS-mutant-specific inhibitors as lumakras or sotorasib (Mottini et al., 2019). Nonetheless, the persistent emergence of drug resistance in cancer therapy poses a significant challenge in the field of oncology.

1.2 Cancer Hallmark: deregulating cellular energetics.

Anabolic processes in cells require a huge amount of ATP, and normal cells meet this need through chemiosmosis which takes place in mitochondria. In normal cells, in the presence of oxygen, pyruvate after glycolysis is oxidized to acetyl-coenzyme A and enters the Krebs cycle in the mitochondrion to produce electron carriers such as NADH and FADH2 which are further used to make ATP through oxidative phosphorylation. This enables the cell produce 15 times more ATP than in fermentation. Oxidative phosphorylation in mitochondrion is achievable due to compartmentalization of mitochondria to intermembrane space and matrix by outer and inner mitochondrial membranes. This separation allows the mitochondrion to build proton gradient which in turn is responsible for ATP generation (Alberts et al., 2015). But cancer cells switch to the aerobic glycolysis also known as Warburg effect resulting in high glucose uptake and decreased oxygen consumption even in normoxic conditions. As a result, cancer cells ferment pyruvate to lactate, accumulation of which can contribute to cancer development (Vaupel et al., 2019). There are several pros to switching on the aerobic glycolysis for cancer cells:

1. The rate of glucose consumption and accordingly ATP generation is approximately 100 times higher in cancer cells than in normal cells mitochondria due to the aerobic glycolysis (Pfeiffer et al., 2001);
2. Reprogramming of biosynthetic pathways switching on the glycolytic intermediates needed for cancer cells through switching on the M2 isoform of pyruvate kinase (Mazurek et al., 2005);
3. The final product of glycolysis - lactate is an important oncometabolite, which can inhibit anti-tumor immune response, resist to apoptosis, metastasis, and might have withstand to radiotherapy due to it's antioxidative features (Mayer et al., 2013).

In case of KRAS cancer cells, growth factor signaling pathway is upregulated which results in elevated glycolytic flux (Mayers et al., 2016). The benefit of an increased glycolytic flux is that it supplies with glycolytic intermediates to fuel the pentose phosphate pathway, leading to enhanced production of nucleotides and phospholipids essential for the rapid growth and proliferation of cancer cells. This metabolic advantage is particularly significant in KRAS-mutant cancers due to their dependency on glucose (Yun et al., 2009). Also, KRAS-mutant cancer cells have elevated glucose uptake through the GLUT1 glucose transporters to furnish aerobic glycolysis with the substrate (Chun et al., 2010).

Further changes in cellular signaling result in elevated reactive oxygen species (ROS) production, providing a favorable environment that promotes the development of KRAS-mutant cancers. ROS generation by mitochondria plays a crucial role in KRAS mediated cancer proliferation (Weinberg et al., 2010). However, KRAS-mutant cancer cells try to counteract the elevated ROS production, by elevation the level of major antioxidants (catalase, peroxiredoxin 3) and downregulation of the glutathione (GSH) concentrations in the cell (Chun et al., 2010). Nevertheless, cytotoxic effect can be observed in KRAS mutant cells because of its sensitivity to oxidative stress in the absence of glucose in extracellular environment. In KRAS-mutant cancer cells which already try to stabilize their redox state, exhaustion of extracellular glucose initiates positive-feedback loop which includes ROS, tyrosine-kinase signaling, and tyrosine-phosphatases inhibited by ROS. The outcome of this mechanism is the cell death as a result of suicidal ROS production (Graham et al., 2012).

1.3 Combinatorial effect of ATO/VC.

Ascorbic acid or Vitamin C (VC) is a water-soluble vitamin and antioxidant found in various fruits and vegetables. VC is crucial element of many cellular processes, and its deficiency is associated with an increased risk of cancer mortality (Ullah et al., 2012). High doses of VC have shown anticancer abilities in vitro, being non-toxic to normal cells but highly toxic to certain tumor cell lines (Cameron & Pauling, 1976). While early studies demonstrated positive outcomes in cancer patients treated with high-dose VC, recent clinical trials have shown limited efficacy (Yun et al., 2015). The mechanism of cytotoxic action on KRAS cancer cell lines was explained by epigenetic regulation, hypoxia signaling, and intracellular iron metabolism (Kaźmierczak-Barańska et al., 2020). When VC gets oxidized outside of the cell, it forms dehydroascorbate (DHA). Cancer cells absorb DHA instead of glucose due to the structure similarity since their altered metabolism triggers high expression of GLUT1 (glucose transporters). Therefore, GLUT1 transporters in KRAS mutant cancer cells facilitate DHA entry to the cytoplasm where it is converted back to Vitamin C by glutathione (GSH) oxidation (Aguilera et al., 2016). The oxidized form of GSH (GSSG) induces ROS accumulation, and inhibition of glyceraldehyde 3-phosphate dehydrogenase (GAPDH) which in turn is a key producer of ATP by substrate-level phosphorylation. This specific cytotoxicity by ATP shortage was observed in KRAS mutant cancer cells, but not in wild type KRAS (Yun et al., 2015). The redox damage caused by VC also

contributes to inhibited phosphorylation of ERK1/2 and PKM2 which in turn inhibits Warburg effect (Aguilera et al., 2016), mitochondrial metabolic dysregulation (Cenigaonandia-Campillo et al., 2021), and inhibition of metastasis (Wilkes et al., 2018), in KRAS-mutant cancers.

ATO is well-known anti-tumor drug to treat several diseases as anemia, Hodgkin's disease, leukemia, and others (Aronson et al. 1994; Kwong et al., 1997;). The toxicity of ATO is driven by redox reactions with thiol groups of cysteine amino acid residues on various proteins (Bak et al., 2017). Consequently, ATO is potential hazard to many sites as an anticancer therapy: it can block glycolysis through hexokinase 2 or pyruvate kinase 2 (Wong et al., 2013; Zhang et al., 2015); able to induce non-conventional apoptotic pathways (An et al., 2021); induce arrest of cell cyle (Eyvani et al., 2016) and many other processes.
However, the major thiol which is affected by ATO in the cytosol is the glutathione. It binds to arsenic and neutralizes ATO. On the contrary, high levels of ATO oxidizes more GSH, unbalancing redox state of the cell (Hayakawa et al., 2005). Second major target is ROS mediated mitochondrial apoptosis through various by-products in face of radicals (H_2O_2, O_2^{-}•, •NO and others) (Palmeira et al., 2019).

Proposed synergistic action of ATO and VC involves a two-step process: VC depletes glutathione, reducing the cellular antioxidative shield, and ATO effectively attacks thiol-reactive rich groups on iron-sulfur (Fe-S) clusters within mitochondrial oxidative phosphorylation complexes, leading to suicidal ROS production by mitochondria and apoptosis (Burska et al., 2022).

1.4 ATO/D-VC Treatment in AK 192 Cell Line.

The rare finding was made when isomeric analog – D form of Vitamin C (D-VC) showed higher capability in KRAS-mutant tumor xenograft in mice than it's natural L form of Vitamin C (L-VC) (Wu et al., 2020). The potential explanation for this phenomenon is that D-VC has 8 times lower turnover number than it's natural L-VC (Baker et al, 1968). Moreover, the recent paper showed that injection of D-VC to mice had significantly lower toxicity than it's natural form - L-VC while keeping similar effect in producing ROS (Begimbetova & Burska et al., 2024).

The synergistic effect of ATO/D-VC combination was already successfully shown in AK192 $KRAS^{G12D}$ doxycycline inducible mouse pancreatic adenocarcinoma cell line in previous studies

of Begimbetova. After treatment with 5μM ATO and 1 mM D-VC, cell viability and mitochondrial ROS (mROS) production were measured. ATO/D-VC treatment induced significant apoptosis, with approximately 80% cells being positive for PI after 48 hours of treatment, while same concentration of ATO alone showed only ~35% of dead cells (control showed about 20%). In addition, mROS production was 7 times higher in experimental group compared to control group depicting the role of suicidal ROS production by mitochondria (Begimbetova et al., 2022)

1.5 Enforced mitophagy method to study the role of mitochondria in cellular processes.

Mitochondrion is not just a "powerhouse" of the cell. In addition to it's main role in generation of energy and regulation of metabolism, it has other roles: deposition of calcium, inflammation, migration, and aging (Chandel, 2014). Accordingly, it has various mechanisms of quality control (mitodegradome and mitoproteases) which ensure the wellness of mitochondrial organelle (Quirós et al., 2015). Moreover, dysregulation of mitochondrial homeostasis is linked to several diseases (Pickrell et al., 2015; Dorn et al., 2015). Therefore, development of the methodology to study the role of cellular processes with removed mitochondria is essential for understanding the uncertain roles of mitochondrion.

A well-established method to study mitochondrial functions are: culturing cells in media with ethidium bromide to suppress mitochondrial DNA (mtDNA) replication (King et al., 1996); using a restriction endonuclease specifically targeted to mitochondria (Kukat et al., 2008); or by mutating the catalytic subunit of mitochondrial DNA polymerase (Jazayeri et al., 2003). However, all these methods are end up in producing ρ^0 cells, which destroy mtDNA but leaving other mitochondrial functions intact (Jakobson et al., 1993). In comparison to the abovementioned methods, enforced mitophagy method described by João F Passos and his team allows us to investigate cellular functions with eliminated mitochondria. This method implies heterologous expression of the ubiquitin E3 ligase Parkin, combined with short-term mitochondrial uncoupler treatment (CCCP) to achieve low-detectable or undetectable levels of mitochondria in cells (Correia-Melo et al., 2017).

PTEN-induced putative kinase 1 (PINK1)/Parkin-mediated mitophagy is the best understood mechanism of mitochondria-targeted autophagy (Riley, Joel S. and Tait et al., 2016). In this mechanism (Figure 2), the selective removal of damaged or dysfunctional mitochondria, relies on the interaction between PINK1 (Ser/Thr kinase) and Parkin proteins (E3 ubiquitin ligase) (Youle et al., 2011). PINK1 undergoes degradation in healthy mitochondria, but mitochondrial function disruptions lead to accumulation of PINK1 on the outer membrane (Jin et al., 2010). This accumulation stimulates the phosphorylation of ubiquitin and Parkin, activating the Parkin E3 ubiquitin ligase. Then, Parkin ubiquitinates mitochondrial substrates, enhancing PINK1 substrate phosphorylation and Parkin activity (Koyano et al., 2014). The ubiquitinated mitochondria are then targeted for autophagy (Correia-Melo et al., 2017). Therefore, this method is simply based on Parkin overexpression in cells, and mitophagy is induced as a result of mitochondrial membrane potential dysregulation after addition of CCCP.

This method was successfully used to show that mitochondrial depletion can inhibit cell senescence by decreasing pro-inflammatory and pro-apoptotic signals (Correia-Melo & Marques et al., 2016); and programmed necrosis is not affected by the presence or absence of mitochondria in the cell (Tait et al., 2013).

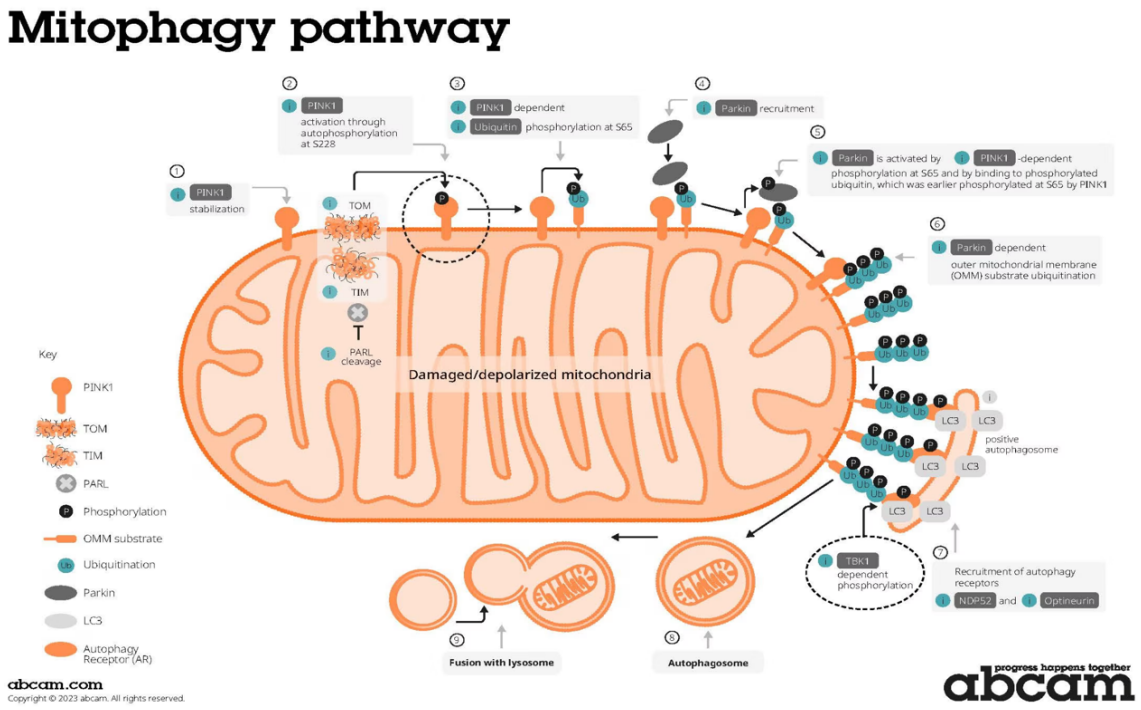

Figure 2. Overview of PINK1-Parkin mediated mitophagy pathway of damaged mitochondria (Mitophagy pathway. Abcam. (2024, March 21). (https://www.abcam.com/neuroscience/mitophagy-pathway)

1.6 Aims and Hypothesis

The **hypothesis** of this thesis project is that ATO/D-VC has significant cytotoxic effect on AK192 cancer cells with functional mitochondria, but does not induce apoptotic cell death in mitochondria deprived cells.

To test this hypothesis, two aims were set:

Aim 1. Establish mitochondria depleted AK192 cell line.

Aim 2. Compare cell viability in AK192 cell lines with and without mitochondria under treatment with combination of oxidative drugs ATO and D-VC.

2 Materials and Methods

2.1 Rationale.

Materials and methods were chosen to fulfil the abovementioned aims. As noted in the aim 1, cell line that will not contain the mitochondria was generated using the AK192 cells. It can be achieved by enforced mitophagy method, which includes overexpression of Parkin ubiquitin E3 ligase and inducing temporary mitochondrial depolarization with uncoupler of mitochondrial ETC to start mitophagy processes in cells (Correia-Melo et al., 2017). Further, they were validated for the absence of mitochondria with western blot assay. Accordingly, to aim 2, apoptosis assay was performed on AK192 cells with and without mitochondria under ATO/D-VC treatment (Begimbetova et al., 2022). For that purpose, we used Annexin V/Propidium Iodide staining by Flow Cytometry to compare the degree of apoptosis.

2.2 Experimental Plan

2.2.1 Step 1: Generation of HA-parkin-expressing AK cells.

The cell line which was used are mouse AK192 pancreatic adenocarcinoma cells which express Tet-On inducible form of $KRAS^{G12D}$ provided from the original sources by Drs. Haoqiang Ying. They were selected based on the previous work which described synergistic effect of ATO/D-VC (Begimbetova et al., 2022). This protocol explains the generation of AK cells with heterologous overexpression of the ubiquitin E3 ligase Parkin (AK-parkin cells).

1) Transformation. E. coli bacterial strain DH5alpha was transformed with pMXs-IP HA-Parkin (Figure 3) (Addgene plasmid # 38248; http://n2t.net/addgene:38248; RRID: Addgene_38248) using heat shock method. Then, one colony from the plate was picked up and grown in 10 ml of LB (lysogeny broth) with addition of 100 ug/ul ampicillin (Sigma Aldrich) as a selection marker, since the plasmid contains ampicillin resistance gene (AmpR). Finally, plasmid was purified by HiPure Plasmid Miniprep Kit (ThermoFisher) for the transfection.

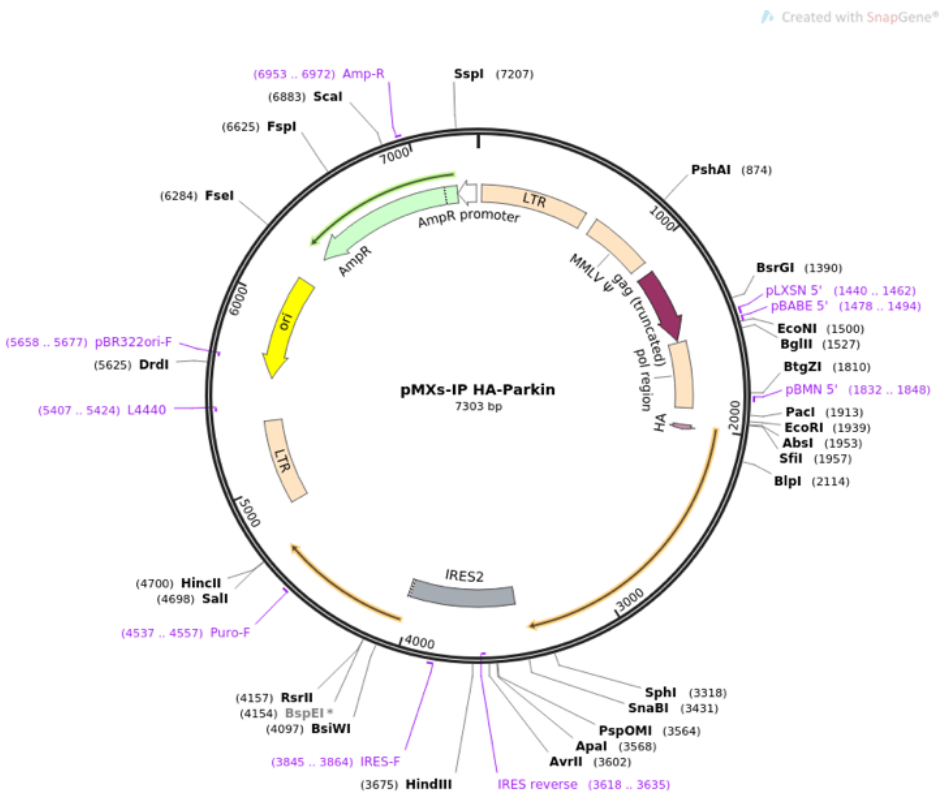

Figure 3. Plasmid of pMXs-IP HA-Parkin (Addgene plasmid # 38248; http://n2t.net/addgene:38248; RRID: Addgene_38248).

Before transfection, restriction analysis was performed to confirm that plasmid which was transformed into bacteria is indeed a pMXs-IP HA-Parkin.

2) Transfection. Parkin plasmid was co-transfected with pCL-Ampho retrovirus packaging vector with Lipofectamine 3000 Transfection reagent (ThermoFisher) in Reduced-Serum Medium (DMEM/F-12 basal medium with reduced FBS) to minimize interference. $3x10^9$ HEK 293T cells were seeded in a 6 cm plate for transfection. After 24 hours the media was changed to 30% FBS (Capricorn Scientific, Germany) complete DMEM/F-12 (US Biological Life Sciences, USA).

3) Transduction was performed 72 hours after transfection (48 hours after changing the media). For this purpose, media was collected and filtered with a 0.45 um PVDF syringe filters (to filter out viruses from cellular compartments). Then, AK192 cells were infected with 1 ml of virus suspension in combination with Polybrene infection reagent (Sigma-Aldrich) 8 ug/ul. Polybrene is a cationic polymer to enhance efficiency of infection by neutralizing the negative charge on the viral and cellular surfaces. Transduction was repeated 6 hours after the first one. The next day

transduction was followed by selection with puromycin dihydrochloride (Sigma-Aldrich, analog of the 3′ end of aminoacyl-tRNA) at the concentration of 2 ug/ul.

2.2.2 Validation of HA-Parkin expression in transduced cells.

To confirm the presence of Parkin western blotting against HA tagged parkin proteins in transduced cells was performed. Primary antibodies which were used were Rabbit anti-HA Tag Antibody (BETHYL). Secondary antibodies used were IRDye 680RD Secondary Goat Anti-Rabbit IgG (LI-COR) and the signal was detected using Odyssey CLx Imaging System (LI-COR). The total lysate of the cells was obtained with the help of RIPA (Radioimmuno-precipitation Assay) Lysis Buffer and Bioruptor Plus Sonication System (Diagenode). This buffer is widely used for effective and quick solubilization of proteins and reduces its non-specific binding. Components of RIPA lysis buffer:

- 10mM Tris-HCl, pH 8.0 (buffering agent);
- 1mM EDTA (chelating agent);
- 0.5mM EGTA (chelating agent);
- 1% Triton X-100 (non-ionic detergent);
- 0.1% Sodium Deoxycholate (bile-salt detergent);
- 0.1% SDS (anionic detergent);
- 140mM NaCl (maintains protein solubility);
- Add protease and phosphatase inhibitor cocktail immediately before use (prevent proteolytic degradation).

Total lysate preparation: Cells were washed 2 times with cold PBS, then 330 ul of RIPA was added to the plate and scrapped to the 1.5 ml centrifuge tube. After 20 minutes of incubation on shaker at 4C, samples were sonicated using Bioruptor with high mode for 4 cycles (sonication cycle: 15 sec ON, 30 sec OFF). Protein concentrations were measured and diluted to 4ug/ul with Bradford Protein Assay. Then, lysate was denatured by addition of Laemmli buffer and heating at 95C for 15 minutes.

SDS-PAGE gel electrophoresis: boiled samples were then loaded on the gel (stacking 4%, running 10%) in TGS (Tris-glycine-SDS) buffer and run initially at 120mV, then switched to the 200mV when samples crossed border of the stacking gel.

Western Blotting: separated proteins were transferred to the Immobilon-P PVDF membrane (Merck Millipore) in a CAPS buffer. Then membrane was blocked with 5% milk in PBS-Tween solution for 1 hour at room temperature on shaker. After the blocking, membrane was washed 3 times with PBS-T, and left overnight in primary antibodies (1: 2000) at 4C. On the next day, after washing 3 times with PBS-T, it was left for 2 hours in secondary antibodies (1:5000). After 3 washing steps, images were taken with Odyssey CLx Imaging System.

2.2.3 Step 2: Mitochondrial depletion in AK-parkin cells.

1) Optimization of Carbonyl cyanide m-chlorophenyl hydrazone (CCCP) treatment. To reach this aim, cells were treated with the different concentrations (5-30 uM) of CCCP (Sigma-Aldrich) diluted in DMSO. CCCP is the key element of enforced mitophagy method to disrupt intermembrane potential of mitochondria. It is a lipophilic compound and an uncoupler of mitochondria that disrupts proton gradient in the inner mitochondrial membrane. This depolarization initiates process of mitophagy. On the other hand, CCCP on it's own is a toxic compound to the cell. Therefore, optimizing concentration of CCCP is an important step. We used microscopy, cell count, and TMRE staining to find out optimal concentration of CCCP. Toxicity of the CCCP on cell morphology was visualized through ZEISS Primovert Inverted Microscope (Zeiss, Oberkochen, Germany). 10 nM TMRE is employed to detect changes in mitochondrial membrane potential since it accumulates in acidic environment created by electron transport chain. We observed the changes using ZOE Fluorescent Cell Imager (Bio-Rad). Cell number was counted using Multisizer Coulter Counter 4e (B43905, Beckman Coulter, Life Sciences). The machine works on principle that it measures the size and number of cells by electric impedance created during the flow of cells through an aperture.

Another important point regarding CCCP is to seed cells in the DMEM F-12 containing 1% fetal bovine serum (FBS), rather than in usual 10% because it was shown in previous works that lowering the concentrations of FBS in the cell culture media is key to facilitate PINK1 accumulation at damaged mitochondria (Soutar et al., 2019). After the depletion, media should be changed to DMEM F-12 + uridine (50 ug/ml) (Sigma-Aldrich), because absence of mitochondria will affect the function of the mitochondrial enzyme dihydroorotate dehydrogenase, which is involved in pyrimidine synthesis, and one way to overcome this is through the addition of Urd directly to the medium. We will further use AK(-mito) to depict AK-parkin cells treated with CCCP for 16 hours.

2.2.4 Validation of mitochondrial depletion.

The Western blot for UQCRC2 (functional protein in the third complex of electron transport chain) protein was carried out to identify the mitochondrial depletion and the potential mitochondria recovery after long-term cultivation. Primary antibodies used were anti-UQCRC2 (1:1000) (Abcam). Secondary antibodies used were IRDye 800RD Secondary Antibody Donkey Anti-Mouse (1:5000) (LI-COR) and the signal was detected using Odyssey CLx Imaging System (LI-COR). In addition, anti-GAPDH antibodies (Abcam) were used as a loading control. SDS-PAGE and Western blotting were performed as previously described for cells depleted of mitochondria immediately after depletion, 24 hours post-depletion, and 48 hours post-depletion. After the imaging, the same membrane was stripped by Restore Fluorescent Western Blot Stripping Buffer (ThermoFisher) and then conjugated with anti-GAPDH control.

2.2.5 Step 3: Compare cell viability of ATO/D-VC on cells with and without mitochondria.

Apoptotic assay was performed in AK192 and AK(-mito) cells in response to ATO/D-VC treatment with Propidium Iodide (Invitrogen) and Annexin V - Alexa Fluor® 647 (Invitrogen) using *Attune* NxT *Flow Cytometer* (ThermoFisher). Immediately after depletion, AK(-mito) cells were treated with 1mM D-VC and 5uM ATO. Then, Apoptosis assay Annexin V+PI staining for flow cytometry was performed at 48 hours after ATO/D-VC treatment. All conditions were seeded at a density of 150 000 cells per well on 6 well plates. Protocol below was followed:

1. Prepare a 100 µg/mL working solution of PI by diluting 5 µL of the 1 mg/mL PI stock solution in 45 µL 1X ABB (annexin binding buffer). Keep in the dark before use (in dark 4C for long term storage)
2. From 6 well plate collect DMEM with floating dead cells from each well into a labelled tube.
3. Wash well on the plate with 1 ml PBS, combine the washout with the DMEM in the respective tubes.
4. Trypsinize with 350ul 1X trypsin for 5 min in 37C, stop by adding 650ml of fresh DMEM. Collect cells to the relevant tube to combine with its dead cell/dmem part.

5. Count cells using 500ul of collected cell suspension on Multisizer4e. Calculate total cell count in your total volume collected (-500ul) from each well and centrifuge 5min at 500rcf. Remove DMEM.

6. Wash cells twice with cold PBS and then resuspend pellet gently in Annexin V Binding Buffer AAB at a concentration of $1x10^6$ cells/mL.

7. Transfer 100 µL of cell suspension in a new test tube.

8. Add 5 µL of Alexa Fluor® 647 Annexin V.

9. Add 1 µL of PI solution (from 100 µg/mL stock)

10. Very gently vortex or mix with pipette the cells and incubate for 15 min at RT (25°C) in the dark.

11. Add 400 µL of Annexin V Binding Buffer to each tube. Keep tubes on ice in the dark until analyzed by *Attune* NxT *Flow Cytometer*.

2.3 Statistical analysis

Cell count and sizes were calculated by Multisizer Coulter Counter 4e (B43905, Beckman Coulter, Life Sciences). Intensity of the Western Blot bands were measured by Odyssey CLx Imaging/Scanning System (LI-COR). All other statistical analyses and calculations were performed by GraphPad Prism 8 (San Diego, California, USA).

3 Results

3.1 AK-parkin overexpressing cell line

First of all we transformed HA-Parkin plasmid (Figure 3) into bacteria and then selected the transformed ones by addition of ampicillin. To prove that plasmid which was transformed into E. coli is our HA-Parkin, restriction analysis was performed (Figure 4).

Molecular weight of plasmid is 7303 bp, and when it is digested with EcoRI (only 1 site of restriction), we obtain a distinct band between 8 and 6 kb. When it is double digested (EcoRI and HindIII) we see two bands of molecular weight approximately 5 kb and 2 kb which also corresponds to restriction sites of these enzymes in pMXs-IP HA-Parkin Restriction sites of EcoRI and HindIII are 1939 and 3675 correspondingly, then 3675-1939=1736 is molecular mass for small fragment, and 7303-1736=5567 is molecular mass for large fragment.

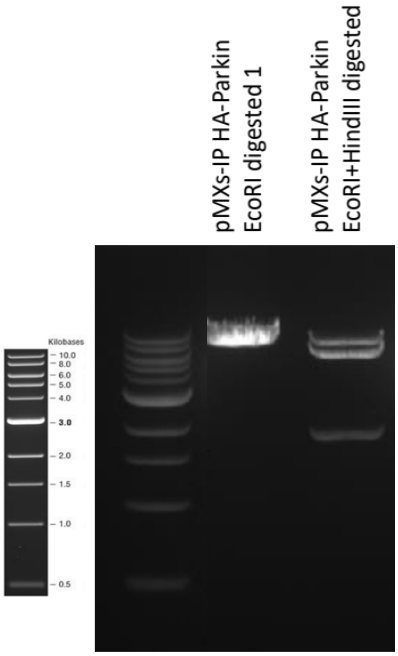

Figure 4. Agarose gel electrophoresis for the patterns obtained after restriction of the amplified DNA of pMXs-IP HA-Parkin plasmid in AK cells with restriction enzymes.

Then, after transduction of AK192 cells (AK-Parkin cells), we were also required to validate that AK-Parkin cells are certainly express protein of our interest. To show it, Western Blot was performed against HA-tag (Figure 5). The molecular weight of Parkin is 52 kDa.

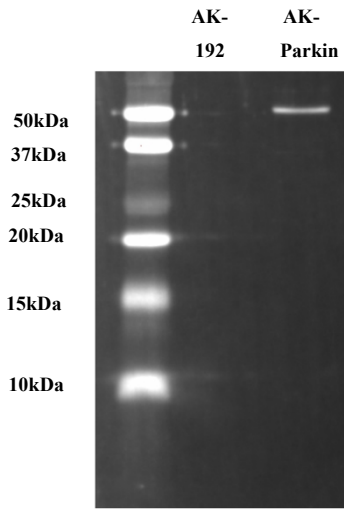

Figure 5. Western Blot showing HA tagged proteins in our cells performed in 10% polyacrylamide gel. This picture illustrates the ectopic expression of introduced Parkin protein in AK-Parkin cells.

3.2 Mitochondrial depletion of AK-Parkin cells

Further to find optimal conditions for the depletion of mitochondria in AK-Parkin cells, the AK-Parkin cells were titrated with CCCP in the range between 5 uM - 30 uM for 16h in DMEM containing 1% FBS (Fig. 6), because in previous works was shown that lowering the concentrations of FBS in the cell culture media is key to facilitate PINK1 accumulation at damaged mitochondria (Soutar et al., 2019). Then, cells were morphologically analyzed either immediately after depletion, or 24 hours incubation in DMEM F-12 + uridine.

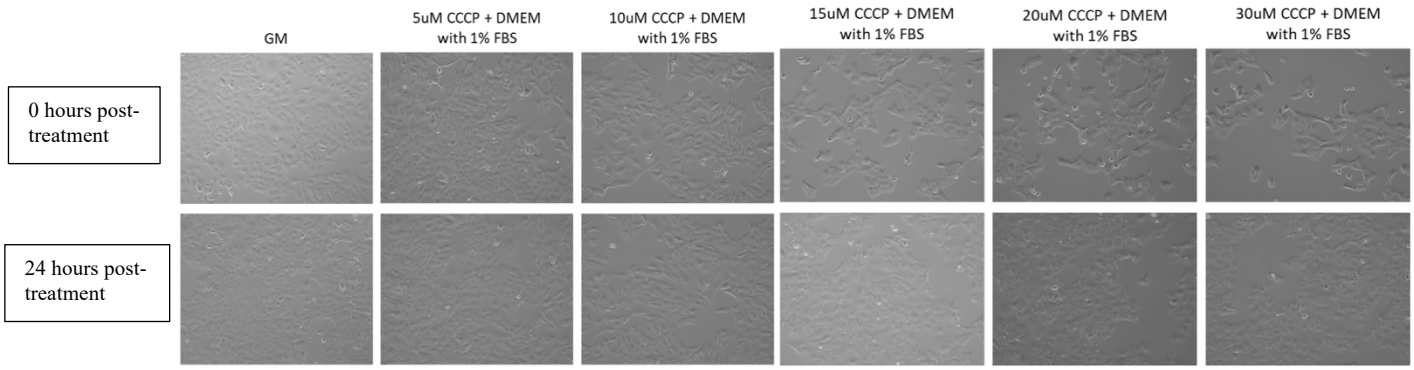

Figure 6. Effect of 5-30 uM concentrations of CCCP on the morphology of AK192-parkin cells. Images were taken with ZEISS Primovert Inverted Microscope (Zeiss, Oberkochen, Germany).

From the pictures present on Figure 6, for further investigations were chosen 5 and 10 uM concentrations of CCCP. These 2 concentrations were set because starting from 15 uM CCCP

addition to AK-Parkin cells, it causes some morphological changes as elongation of cells and some toxicity.

Then cells treated with above mentioned concentrations (5 and 10 uM), were stained with TMRE (this dye accumulates only in functionally active mitochondria) and Hoechst (to stain the nucleus localization). This combination was used for the determination of effective mitochondrial depolarization after CCCP incorporation to the cells. TMRE depicts changes in mitochondrial membrane potential and therefore is useful to identify whether mitochondria in cells are depolarized to induce PINK1 accumulation and start mitophagy process. Hoechst staining also supports us with the insights regarding mitochondrial and nuclear colocalization alterations. Pictures were taken at 4 time points: immediately after the depletion, and incubation at 24, 48 and 72 hours after depletion (Figure 7). Cells were grown in DMEM F-12 + uridine media after the depletion.

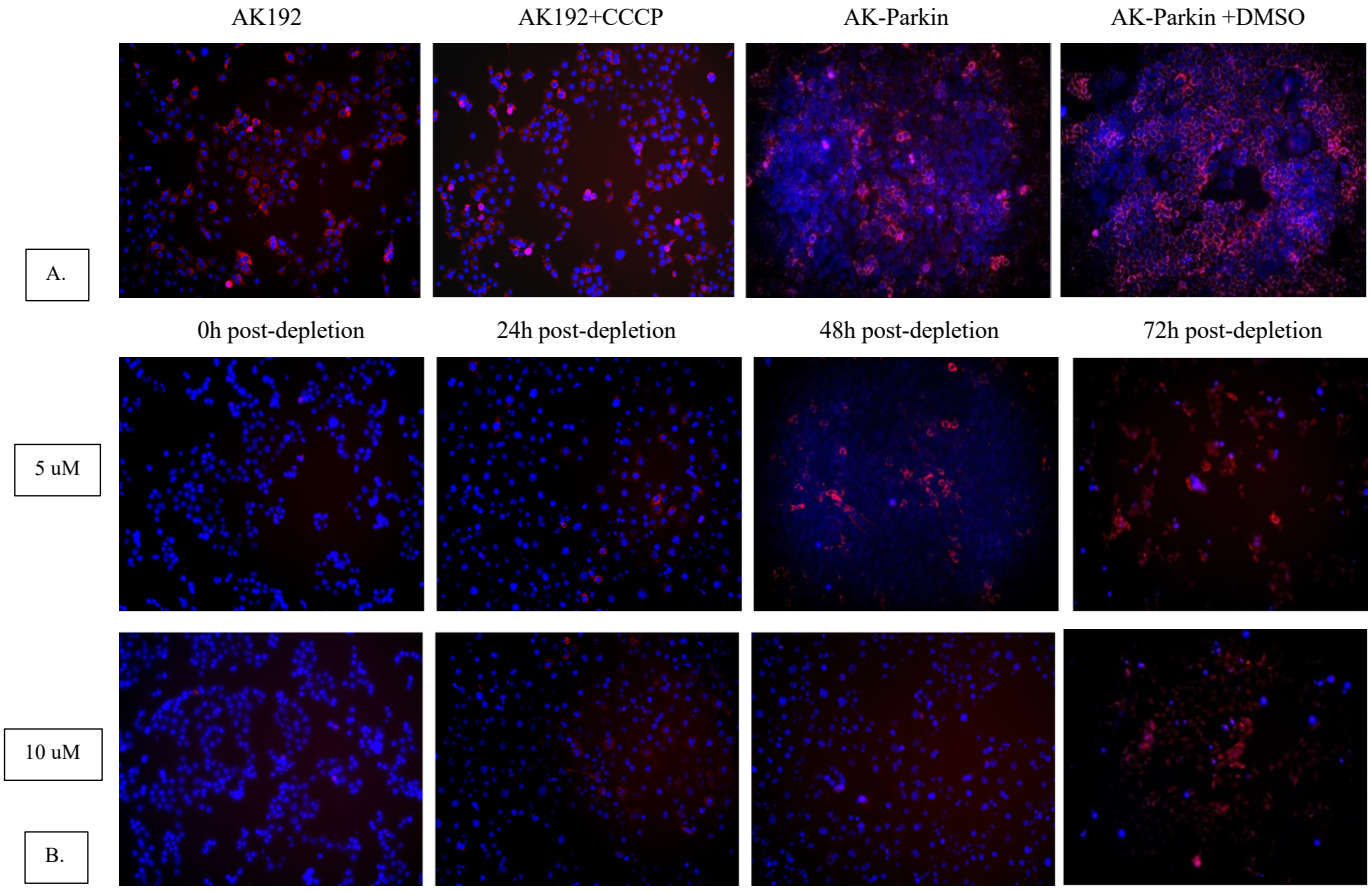

Figure 7. Representative images of TMRE signal for AK192 and AK-Parkin cells with and without addition of CCCP. (A)AK192 and AK-Parkin controls, and (B) AK-Parkin cells treated either with 5 or 10 uM CCCP for 72 hours. Images were taken by ZOE Fluorescent Cell Imager (Bio-Rad) from different spots.

ZOE Fluorescent Cell Imager using TMRE staining shows that both 5 and 10uM CCCP concentrations induce mitochondrial intermembrane depolarization immediately after addition of the ionophore. At 24 hours after depletion, mitochondria are still depolarized, but starting from 48 hours post-depletion, mitochondria started to recover in cells treated with 5 uM, whether signal was not detected in cells treated with 10 uM CCCP. Signal at 72 hours at both concentrations comes mostly from the dead cells. However, normal AK192 and AK-Parkin when not treated with CCCP, and a negative control group (AK-Parkin+DMSO) did not show mitochondrial membrane depolarization. In addition, AK192 cells not overexpressing Parkin protein were treated with CCCP for 16 hours and stained immediately with TMRE did not show decrease in the TMRE signal as in CCCP treated AK-Parkin cells depicting disappeared mitochondria.

However, we identified that cells support their viability for a short period of time (Figure 8). Cells were grown in 10% FBS DMEM+uridine, and media was changed every 24 hours to avoid uridine shortage. Nevertheless, cells at 72 hours start to detach and die. This allows us to examine AK(-mito) cells only for 48 hours.

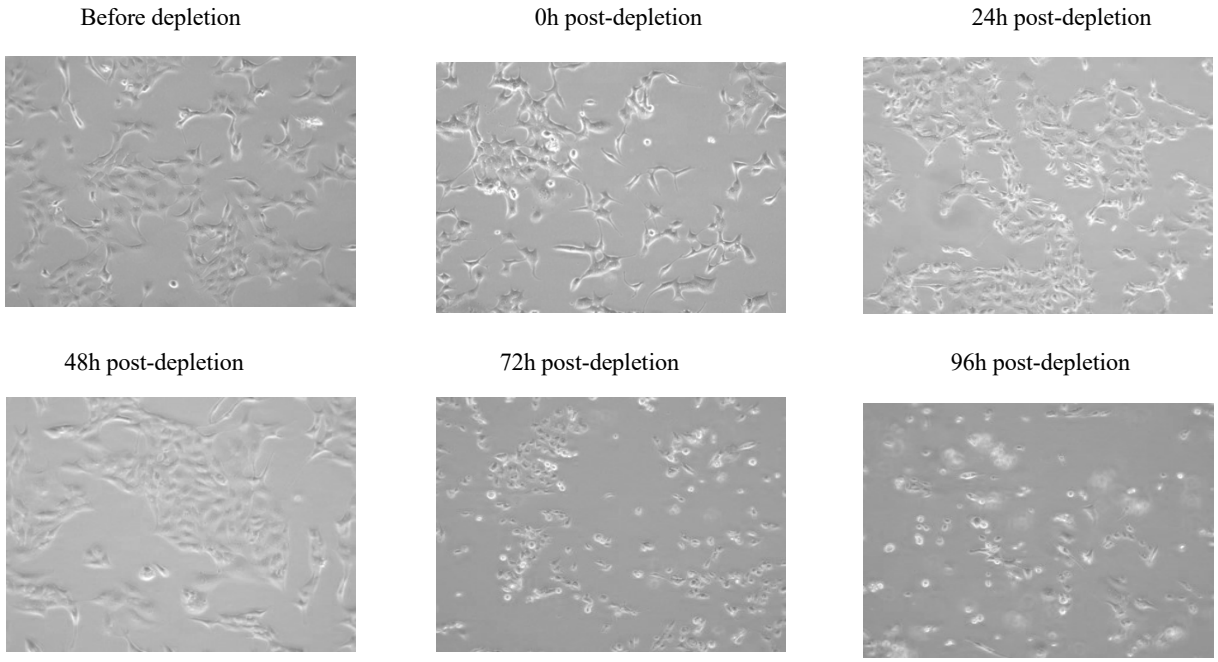

Figure 8. AK(-mito) cells grown in 10% FBS DMEM+uridine media for 96 hours. Images were taken with ZEISS Primovert Inverted Microscope (Zeiss, Oberkochen, Germany).

3.3 Validation of mitochondrial depletion

Next, we investigated mitophagy by mitochondrial marker UQCRC2, antibody used for widespread mitophagy QC assay (Correia-Melo et al., 2017) (Figure 9A). Western Blotting was performed from the total lysates of the above conditions up to 48h growth post-depletion with 10uM CCCP for 16h.

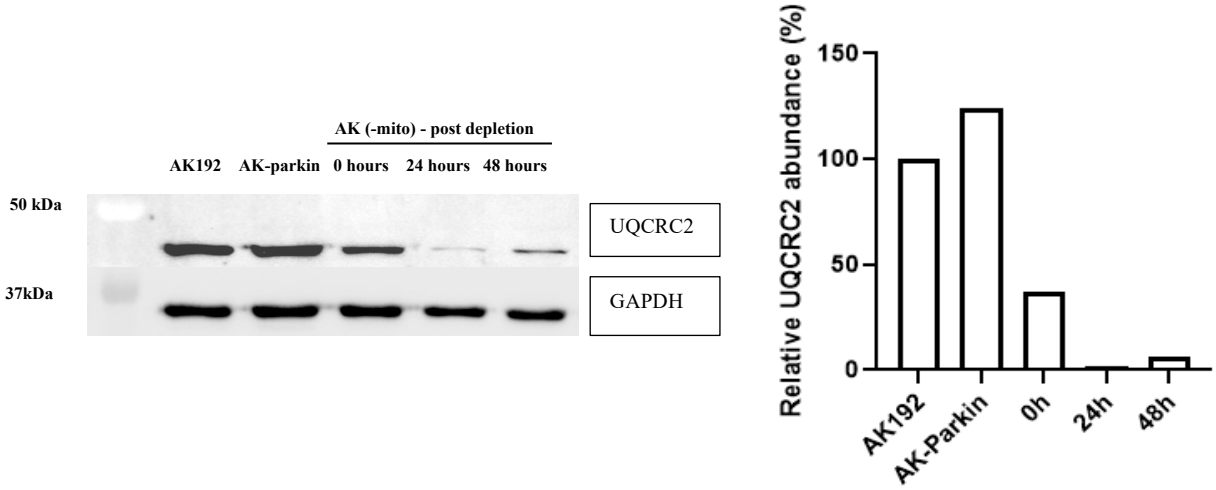

A) B)

Figure 9. The Western blots depicting mitochondrial depletion with mitochondrial marker UQCRC2 in AK192 cell line. A – anti-GAPDH (loading control - 36kDa), and anti-UQCRC2 (48kDa) bands showing dynamic reduction of proteins. B – normalized levels of UQCRC2 to the loading control (GAPDH). Images were taken and quantified with Odyssey CLx Imaging System (LI-COR).

Based on the above Western Blot, we observed the dynamic changes of mitochondrial marker UQCRC2 (Figure 9B). Right after the removal of CCCP, level of UQCRC2 dropped 2.7 times compared to AK192 (~37% relative to control), but after 24 hours of post-depletion the signal was close to be undetectable (1.9% relative to control). 48 hours after depletion, the signal came back, indicating 3.5 times more UQCRC2 levels than at 24 hours (6.67% relative to control). However, AK-Parkin cells showed higher concentration of UQCRC2 in the cell up for 28% compared to AK192.

3.4 Apoptotic responses of AK192 and AK(-mito) to ATO/D-VC

Essential step before comparison the effect of ATO/D-VC to AK192 and AK(-mito) cell lines, was to quantify cell confluency at the moment of the treatment with ATO/D-VC. To test the

impact of ATO/D-VC on cell viability of AK(-mito), 150 000 AK-Parkin cells were seeded on the 6-well plate; then after 24 hours after seeding they were depleted with CCCP for 16 hours; and finally, immediately after depletion they were treated with ATO/D-VC for 48 hours. In comparison, 150 000 AK192 cells were seeded on 6-well plate and after 24 hours after the seeding treated with ATO/D-VC for 48 hours. Since the AK(-mito) cells remain on plate 40 hours at the moment of treatment with ATO/D-VC, while AK192 cells treated with ATO/D-VC 24 hours after the seeding, an important question arises: is there significant difference in cell number at the moment of treatment with drug between AK192 and AK(-mito) cells? To find out the answer for this question, we counted the number of cells at the moment of treatment (Figure 10).

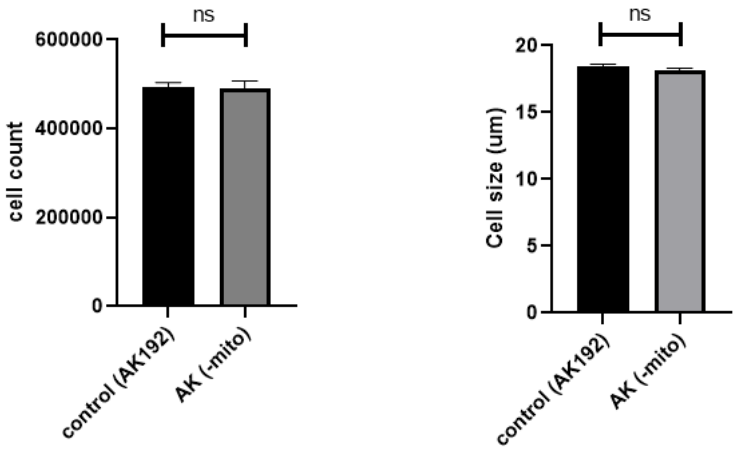

Figure 10. Evaluation of AK192 and AK(-mito) cell numbers and cell size with Multisizer Coulter Counter 4e (B43905, Beckman Coulter, Life Sciences) just before the ATO/D-VC treatment. (AK192 cell count mean – 492820, AK(-mito) cell count mean – 491020; AK192 cell size mean – 18.41 um, AK(-mito) cell count mean – 18.11 um; error bars indicate standard deviation).

Because no difference in cell counts were detected, Annexin V/Propidium Iodide (PI) double staining was performed to analyze apoptosis in AK192 and AK(-mito) cells treated with ATO/D-VC for 48 hours (Figure 11A, 11B). Results illustrate the difference in distribution of cells either for AnnexinV - Alexa Fluor® 647, PI or both. From these graphs we can observe the difference in proportion for alive (AV(-), PI(-)), dead (AV(+), PI(+)), early apoptotic (AV(+), PI(-)), and necrotic cells (AV(-), PI(+)) from 6 independent experiments.

Since we have different viability for AK192 and AK(-mito) cells even without ATO/D-VC treatment, to compare cell viability of AK192 and AK(-mito) cells treated with the drug we treamed and normalized percentage of alive cells respectively to it's appropriate controls (Figure 11C).

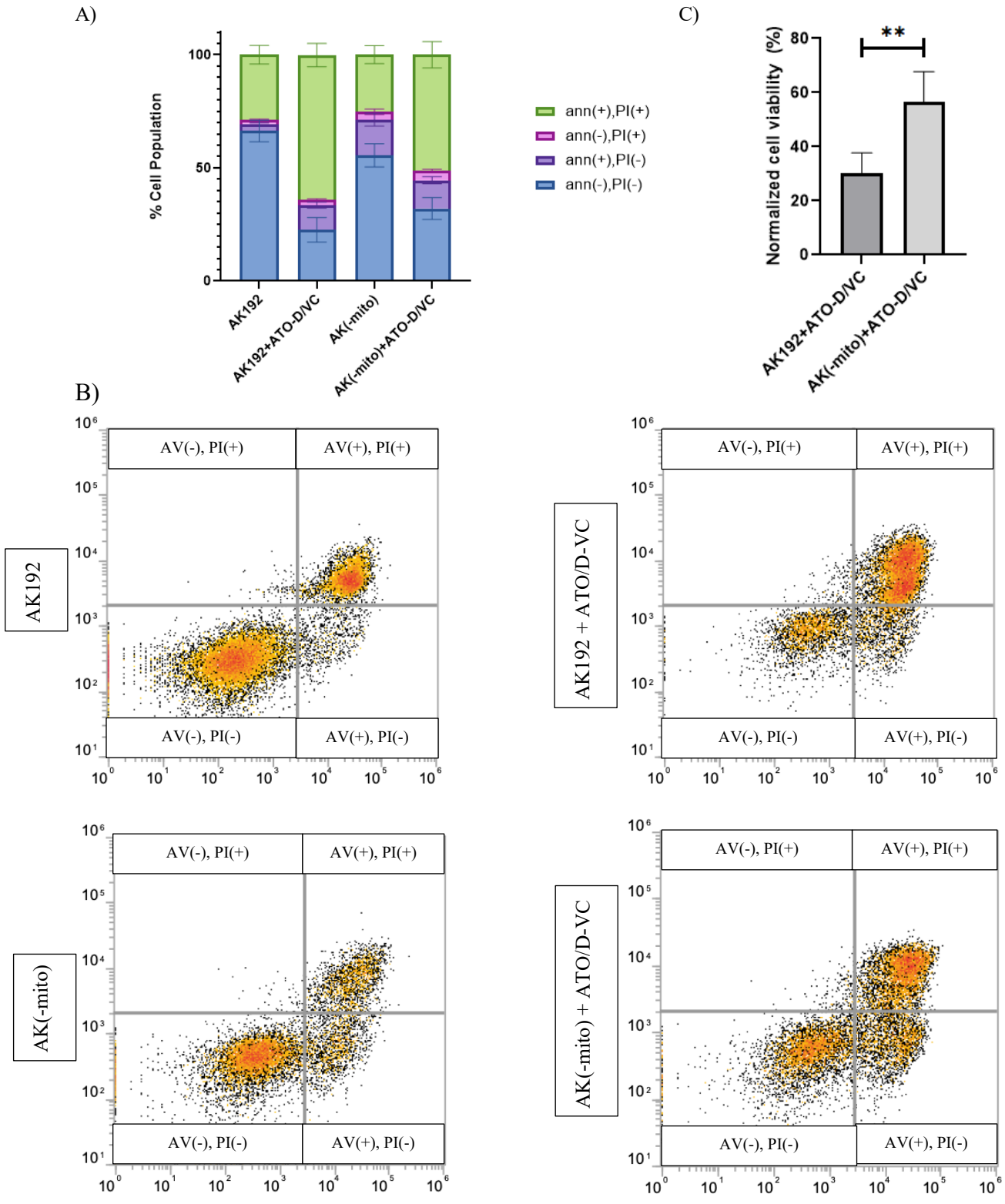

Figure 11. Annexin – PI double staining of AK192 and AK(-mito) cells treated or not with ATO/D-VC. A – distribution of population of cells for annexin and PI status (error bars indicate standard deviation). B – single cell distribution of samples (30 000 events for every condition). C – normalized percentage of alive (AV(-), PI(-)) AK192 and AK(-mito) cells treated with the drug (unpaired, two-tailed t-test; mean of AK192 – 30.17%, mean of AK(-mito) – 56.42%; error bars indicate standard deviation).

4. Discussion

For the first time mitochondria were discovered by Albert Kölliker in 1857, and 100 years later, in 1957 Philip Siekevitz in his paper described the central role of mitochondria in oxidation of food and named them "powerhouse of the cell" (Siekevitz, 1957). Nowadays, we say that "mitochondria are not just a powerhouse of the cell" about the mitochondria. Many other cellular and molecular functions were described to be mediated by the mitochondria in the end of past century: proliferation of the cell, programmed cell death, regulation of second messengers and redox levels, detoxication, heme synthesis, and others (Zorov et al., 1997). In past decades, scientists actively investigated the role of mitochondria as signaling orgenelles (Chandel, 2014), in ageing, diseases (Quirós et al., 2015), and tumorigenesis (Zong et al., 2016). Recently, key element of learning and memory formation – synaptic plasticity shown to be directed by mitochondrial fusion in adult-born neurons (Kochan et al., 2024).

As a result, defining the active role of mitochondria is an important step in in understanding above mentioned processes. Whereas when we are interested in the function of gene of interest in the cell, we analyze it's role through loss-of-function approaches. Alternatively, removal of mitochondria in the cell enables us to study it's cellular functions. As mentioned in the Introduction section, enforced mitophagy method has an advantage in eliminating the whole mitochondrial organelle rather than just disrupting mitochondrial DNA as in other methods (Correia-Melo et al., 2017). This method already was implied to depict the role of mitochondria in necroptosis (Tait et al., 2013) and aging (Correia-Melo & Marques et al., 2016).

Susceptibility of some KRAS mutant cancer cells to VC and ATO were shown previously (Kaźmierczak-Barańska et al., 2020; Burska et al., 2022) as a result of metabolic deregulation due to the GLUT1 overexpression (Chun et al., 2010) to reach Warburg effect and glycolytic flux which support survival of cancel cells (Mayer et al., 2013). The purpose of this research project was to optimize and validate enforced mitophagy method as a useful tool to study the role of mitochondria in cytotoxicity of ATO/D-VC in $KRAS^{G12D}$ AK192 cells.

Here, we could reach partial depletion of mitochondria in AK192 cells (Figure 7, 9), but faced a problem with the viability of the cells after the depletion. Long term culture of mitochondria depleted AK 192 cells was not possible as after 72 hours cells started to die and could not be used for further experiments (Figure 8). In the original paper describing the protocol of depletion and

in studies which used this method, cells were able to survive and grow for a long time after depletion (Correia-Melo et al., 2017; Tait et al., 2013; Correia-Melo & Marques et al., 2016). However, some cell lines don't survive after mitochondrial depletion and it seems to depend on cell-type (Correia-Melo et al., 2017). Probably, AK192 cell line is one of them and they may die due to the incomplete depletion of mitochondria. In similar works with enforced mitophagy, other teams could reach total depletion of mitochondria (MRC5 fibroblasts, HeLa, 3T3-SA< SVEC and so others) (Correia-Melo et al., 2017; Tait et al., 2013; Correia-Melo & Marques et al., 2016). The possible explanation of lethality in case of incomplete depletion is that already ATP exhausted cancer cells try to repopulate their mitochondria. Because mitochondria have "relaxed genome", it's replication does not depend on cell cycle (Birky, 1994), and in attempt to regain the population of mitochondria it probably leads to energy exhaustion and cell death because they still need oxidative phosphorylation to support sufficient amounts of ATP in the cell. To test this hypothesis, we plan try to reach the total depletion in AK192 cells, and observe the consequences.

Previously, Begimbetova and her colleagues showed high cytotoxicity of ATO/D-VC at 48 hours for AK192 cell line (Begimbetova et al., 2022). In addition to this, we optimized depletion condition to get similar cell confluency at the moment of the treatment (Figure 10). Therefore, we were able to compare the cytotoxicity of the drug on control cells and mitochondria depleted cells (Figure 11C) using Flow Cytometry with AnnexinV and PI.

Apoptotic assay showed slightly increased percentage of live cells for AK(-mito) cells than AK192. However, we should consider that depletion of mitochondria was not total, and there were still some mitochondria which were able to generate ROS to trigger apoptosis. Moreover, all the manipulations related to the depletion process also influenced the fitness of cells. These limitations complicate the real estimation of mitochondrial mediated apoptosis by ATO/D-VC. Even so, AK(-mito) cells showed less cell death after ATO/D-VC as compared to response AK192 cells with fully functional mitochondria. The toxicity of ATO/D-VC to mitochondria depleted cells can be explained by the fact that both ATO and D-VC have other modes of actions on cancer cells beyond the mitochondria. ATO is not specific to mitochondrial proteins, it targets thiol groups of different proteins other than mitochondrial proteins (Bak et al., 2017). VC is known to inhibit GAPDH and cause ATP stress in KRAS mutant cancer cells (Yun et al., 2015). In addition, mitochondria are not only source of ROS, endoplasmic reticulum, lysosomes, and peroxisomes are also contribute to production of radicals in the cell.

5. Limitations

This study carries several limitations. First, validation of mitochondrial depletion – similar works with depletion of mitochondria usually perform validation with 3 approaches: western blotting for mitochondrial markers (UQCRC2, TOMM20, SDHA, and NDUFB8), mitochondrial DNA copy number with qPCR (MTRNR2, MTTL1 genes), and immunofluorescence staining by microscopy (Correia-Melo et al., 2017). However, in this work only Western Blotting for mitochondrial marker UQCRC2 and TMRE staining were shown. Secondly, lethality of mitochondria removed cells after 72 hours complicated setting of experiments. Therefore, mitochondria depleted cells immediately after removal of CCCP, were treated with the ATO/D-VC, which also might interfere the results. Thirdly, characterization of AK(-mito) cells could give better understanding of crucial factors such as viability of cells, cell cycle, classical and non-classical cell death and so on. Finally, measurement of ROS production in ATO/D-VC treated AK192 and AK(-mito) cells would gave us more detailed answer regarding the role of suicidal ROS production by mitochondria in this study.

6. Summary and Future Perspectives

We generated AK192 cancer cell line with low-detectable mitochondria and used it to test whether it plays a role in toxicity of ATO/D-VC. AK(-mito) cells had up to 2 times higher survival than AK192 when treated with ATO/D-VC supporting the hypothesis that mitochondria play a considerable role in cytotoxicity of ATO/D-VC in Tet-On inducible $KRAS^{G12D}$ AK192 cells.

To move forward, optimization of depletion process and characterization of cell without mitochondria are in priority. After the establishment of well-depleted and well-characterized cell lines, mitochondrial ROS production by MitoSOX can be done to evaluate it's role. Further, difference between KRAS and non-KRAS cancer cell lines can be planned to evaluate the role of mitochondria as a signaling organelle in KRAS-mediated tumorigenicity (Chandel, 2014; Weinberg et al., 2010)

7. Bibliography

Riley JS, Tait SW. Mechanisms of mitophagy: putting the powerhouse into the doghouse. Biol Chem. 2016 Jul 1;397(7):617-35. doi: 10.1515/hsz-2016-0137. PMID: 27071149.

Correia-Melo C, Ichim G, Tait SW, Passos JF. Depletion of mitochondria in mammalian cells through enforced mitophagy. Nat Protoc. 2017 Jan;12(1):183-194. doi: 10.1038/nprot.2016.159. Epub 2016 Dec 22. PMID: 28005069.

Soutar MPM, Kempthorne L, Annuario E, Luft C, Wray S, Ketteler R, Ludtmann MHR, Plun-Favreau H. FBS/BSA media concentration determines CCCP's ability to depolarize mitochondria and activate PINK1-PRKN mitophagy. Autophagy. 2019 Nov;15(11):2002-2011. doi: 10.1080/15548627.2019.1603549. Epub 2019 May 7. PMID: 31060423; PMCID: PMC6844515.

Tsuchida N, Ryder T, Ohtsubo E. Nucleotide sequence of the oncogene encoding the p21 transforming protein of Kirsten murine sarcoma virus. Science. 1982 Sep 3;217(4563):937-9. doi: 10.1126/science.6287573. PMID: 6287573.

Colicelli J. Human RAS superfamily proteins and related GTPases. Sci STKE. 2004 Sep 7;2004(250):RE13. doi: 10.1126/stke.2502004re13. PMID: 15367757; PMCID: PMC2828947.

Zenonos K, Kyprianou K. RAS signaling pathways, mutations and their role in colorectal cancer. World J Gastrointest Oncol. 2013 May 15;5(5):97-101. doi: 10.4251/wjgo.v5.i5.97. PMID: 23799159; PMCID: PMC3682174.

Russo M, Di Nicolantonio F, Bardelli A. Climbing RAS, the everest of oncogenes. Cancer Discov. 2014 Jan;4(1):19-21. doi: 10.1158/2159-8290.CD-13-0906. PMID: 24402942.

Pantsar T, Rissanen S, Dauch D, Laitinen T, Vattulainen I, Poso A. Assessment of mutation probabilities of KRAS G12 missense mutants and their long-timescale dynamics by atomistic molecular simulations and Markov state modeling. PLoS Comput Biol. 2018 Sep 10;14(9):e1006458. doi: 10.1371/journal.pcbi.1006458. PMID: 30199525; PMCID: PMC6147662.

Vaupel P, Schmidberger H, Mayer A. The Warburg effect: essential part of metabolic reprogramming and central contributor to cancer progression. Int J Radiat Biol. 2019 Jul;95(7):912-919. doi: 10.1080/09553002.2019.1589653. Epub 2019 Mar 22. PMID: 30822194.

Yun J, Rago C, Cheong I, Pagliarini R, Angenendt P, Rajagopalan H, Schmidt K, Willson JK, Markowitz S, Zhou S, Diaz LA Jr, Velculescu VE, Lengauer C, Kinzler KW, Vogelstein B, Papadopoulos N. Glucose deprivation contributes to the development of KRAS pathway mutations in tumor cells. Science. 2009 Sep 18;325(5947):1555-9. doi: 10.1126/science.1174229. Epub 2009 Aug 6. PMID: 19661383; PMCID: PMC2820374.

Weinberg F, Hamanaka R, Wheaton WW, Weinberg S, Joseph J, Lopez M, Kalyanaraman B, Mutlu GM, Budinger GR, Chandel NS. Mitochondrial metabolism and ROS generation are essential for Kras-mediated tumorigenicity. Proc Natl Acad Sci U S A. 2010 May 11;107(19):8788-93. doi: 10.1073/pnas.1003428107. Epub 2010 Apr 26. PMID: 20421486; PMCID: PMC2889315.

Graham NA, Tahmasian M, Kohli B, Komisopoulou E, Zhu M, Vivanco I, Teitell MA, Wu H, Ribas A, Lo RS, Mellinghoff IK, Mischel PS, Graeber TG. Glucose deprivation activates a metabolic and signaling amplification loop leading to cell death. Mol Syst Biol. 2012 Jun 26;8:589. doi: 10.1038/msb.2012.20. PMID: 22735335; PMCID: PMC3397414.

Yun J, Mullarky E, Lu C, Bosch KN, Kavalier A, Rivera K, Roper J, Chio II, Giannopoulou EG, Rago C, Muley A, Asara JM, Paik J, Elemento O, Chen Z, Pappin DJ, Dow LE, Papadopoulos N, Gross SS, Cantley LC. Vitamin C selectively kills KRAS and BRAF mutant colorectal cancer cells by targeting GAPDH. Science. 2015 Dec 11;350(6266):1391-6. doi: 10.1126/science.aaa5004. Epub 2015 Nov 5. PMID: 26541605; PMCID: PMC4778961.

Kaźmierczak-Barańska J, Boguszewska K, Adamus-Grabicka A, Karwowski BT. Two Faces of Vitamin C-Antioxidative and Pro-Oxidative Agent. Nutrients. 2020 May 21;12(5):1501. doi: 10.3390/nu12051501. PMID: 32455696; PMCID: PMC7285147.

Ngo B, Van Riper JM, Cantley LC, Yun J. Targeting cancer vulnerabilities with high-dose

vitamin C. Nat Rev Cancer. 2019 May;19(5):271-282. doi: 10.1038/s41568-019-0135-7. PMID: 30967651; PMCID: PMC6526932.

Kwong YL, Todd D. Delicious poison: arsenic trioxide for the treatment of leukemia. Blood. 1997 May 1;89(9):3487-8. PMID: 9129058.

Palmeira CM, Teodoro JS, Amorim JA, Steegborn C, Sinclair DA, Rolo AP. Mitohormesis and metabolic health: The interplay between ROS, cAMP and sirtuins. Free Radic Biol Med. 2019 Sep;141:483-491. doi: 10.1016/j.freeradbiomed.2019.07.017. Epub 2019 Jul 24. PMID: 31349039; PMCID: PMC6718302.

Burska AN, Ilyassova B, Dildabek A, Khamijan M, Begimbetova D, Molnár F, Sarbassov DD. Enhancing an Oxidative "Trojan Horse" Action of Vitamin C with Arsenic Trioxide for Effective Suppression of KRAS-Mutant Cancers: A Promising Path at the Bedside. Cells. 2022 Nov 1;11(21):3454. doi: 10.3390/cells11213454. PMID: 36359850; PMCID: PMC9657932.

Begimbetova D, Kukanova A, Fazyl F, Manekenova K, Omarov T, Burska AN, Khamijan M, Gulyayev A, Yermekbayeva B, Makishev A, Saliev T, Batyrbekov K, Aitbayev C, Spatayev Z, Sarbassov D. The Oxidative Drug Combination for Suppressing KRAS G12D Inducible Tumour Growth. Biomed Res Int. 2022 Dec 30;2022:9426623. doi: 10.1155/2022/9426623. PMID: 36619305; PMCID: PMC9822755.

Kukat, A., Kukat, C., Brocher, J., Schäfer, I., Krohne, G., Trounce, I. A., Villani, G., & Seibel, P. (2008). Generation of rho0 cells utilizing a mitochondrially targeted restriction endonuclease and comparative analyses. *Nucleic acids research*, *36*(7), e44. https://doi.org/10.1093/nar/gkn124

King, M. P., & Attardi, G. (1996). Isolation of human cell lines lacking mitochondrial DNA. *Methods in enzymology*, *264*, 304–313. https://doi.org/10.1016/s0076-6879(96)64029-4

Jazayeri, M., Andreyev, A., Will, Y., Ward, M., Anderson, C. M., & Clevenger, W. (2003). Inducible expression of a dominant negative DNA polymerase-gamma depletes mitochondrial DNA and produces a rho0 phenotype. *The Journal of biological chemistry*, *278*(11), 9823–9830.

https://doi.org/10.1074/jbc.m211730200

Jacobson, M. D., Burne, J. F., King, M. P., Miyashita, T., Reed, J. C., & Raff, M. C. (1993). Bcl-2 blocks apoptosis in cells lacking mitochondrial DNA. *Nature*, *361*(6410), 365–369. https://doi.org/10.1038/361365a0

Chandel N. S. (2014). Mitochondria as signaling organelles. *BMC biology*, *12*, 34. https://doi.org/10.1186/1741-7007-12-34

Youle, R. J., & Narendra, D. P. (2011). Mechanisms of mitophagy. *Nature reviews. Molecular cell biology*, *12*(1), 9–14. https://doi.org/10.1038/nrm3028

Koyano, F., Okatsu, K., Kosako, H., Tamura, Y., Go, E., Kimura, M., Kimura, Y., Tsuchiya, H., Yoshihara, H., Hirokawa, T., Endo, T., Fon, E. A., Trempe, J. F., Saeki, Y., Tanaka, K., & Matsuda, N. (2014). Ubiquitin is phosphorylated by PINK1 to activate parkin. *Nature*, *510*(7503), 162–166. https://doi.org/10.1038/nature13392

Jin, S. M., Lazarou, M., Wang, C., Kane, L. A., Narendra, D. P., & Youle, R. J. (2010). Mitochondrial membrane potential regulates PINK1 import and proteolytic destabilization by PARL. *The Journal of cell biology*, *191*(5), 933–942. https://doi.org/10.1083/jcb.201008084

Parkin mediates proteasome-dependent protein degradation and rupture of the outer mitochondrial membrane**.** Yoshii SR, Kishi C, Ishihara N, Mizushima N. *J Biol Chem. 2011 Jun 3;286(22):19630-40. Epub 2011 Mar 18.* 10.1074/jbc.M110.209338 PubMed 21454557

Zenonos, K., & Kyprianou, K. (2013). RAS signaling pathways, mutations and their role in colorectal cancer. *World journal of gastrointestinal oncology*, *5*(5), 97–101. https://doi.org/10.4251/wjgo.v5.i5.97

Lemmon, M. A., & Schlessinger, J. (2010). Cell signaling by receptor tyrosine kinases. *Cell*, *141*(7), 1117–1134. https://doi.org/10.1016/j.cell.2010.06.011

Janknecht, R., Ernst, W. H., Pingoud, V., & Nordheim, A. (1993). Activation of ternary complex

factor Elk-1 by MAP kinases. *The EMBO journal*, *12*(13), 5097–5104. https://doi.org/10.1002/j.1460-2075.1993.tb06204.x

Roberts, P., Der, C. Targeting the Raf-MEK-ERK mitogen-activated protein kinase cascade for the treatment of cancer. *Oncogene* **26**, 3291–3310 (2007). https://doi.org/10.1038/sj.onc.1210422

Chen X, Thakkar H, Tyan F, Gim S, Robinson H, Lee C, et al. Constitutively active Akt is an important regulator of TRAIL sensitivity in prostate cancer. *Oncogene* (2001) **20**:6073–7. doi:10.1038/sj.onc.1204736

Porta, C., Paglino, C., & Mosca, A. (2014). Targeting PI3K/Akt/mTOR Signaling in Cancer. *Frontiers in oncology*, *4*, 64. https://doi.org/10.3389/fonc.2014.00064

Battaglioni, S., Benjamin, D., Wälchli, M., Maier, T., & Hall, M. N. (2022). mTOR substrate phosphorylation in growth control. *Cell*, *185*(11), 1814–1836. https://doi.org/10.1016/j.cell.2022.04.013

Wang, Y., Kaiser, C. E., Frett, B., & Li, H. Y. (2013). Targeting mutant KRAS for anticancer therapeutics: a review of novel small molecule modulators. *Journal of medicinal chemistry*, *56*(13), 5219–5230. https://doi.org/10.1021/jm3017706

Mottini, C., Tomihara, H., Carrella, D., Lamolinara, A., Iezzi, M., Huang, J. K., Amoreo, C. A., Buglioni, S., Manni, I., Robinson, F. S., Minelli, R., Kang, Y., Fleming, J. B., Kim, M. P., Bristow, C. A., Trisciuoglio, D., Iuliano, A., Del Bufalo, D., Di Bernardo, D., Melisi, D., … Cardone, L. (2019). Predictive Signatures Inform the Effective Repurposing of Decitabine to Treat KRAS-Dependent Pancreatic Ductal Adenocarcinoma. *Cancer research*, *79*(21), 5612–5625. https://doi.org/10.1158/0008-5472.CAN-19-0187

Ostrem, J., Peters, U., Sos, M. *et al.* K-Ras(G12C) inhibitors allosterically control GTP affinity and effector interactions. *Nature* **503**, 548–551 (2013). https://doi.org/10.1038/nature12796

Molecular biology of the cell / Bruce Alberts, Alexander Johnson, Julian Lewis, David Morgan, Martin Raff, Keith Roberts, Peter Walter (2015) ; with problems by John Wilson, Tim Hunt. -- Sixth edition.

Pfeiffer, T., Schuster, S., & Bonhoeffer, S. (2001). Cooperation and competition in the evolution of ATP-producing pathways. *Science (New York, N.Y.)*, *292*(5516), 504–507. https://doi.org/10.1126/science.1058079

Mazurek, S., Boschek, C. B., Hugo, F., & Eigenbrodt, E. (2005). Pyruvate kinase type M2 and its role in tumor growth and spreading. *Seminars in cancer biology*, *15*(4), 300–308. https://doi.org/10.1016/j.semcancer.2005.04.009

Mayer, A., & Vaupel, P. (2013). Hypoxia, lactate accumulation, and acidosis: siblings or accomplices driving tumor progression and resistance to therapy?. *Advances in experimental medicine and biology*, *789*, 203–209. https://doi.org/10.1007/978-1-4614-7411-1_28

Mayers, J. R., Torrence, M. E., Danai, L. V., Papagiannakopoulos, T., Davidson, S. M., Bauer, M. R., Lau, A. N., Ji, B. W., Dixit, P. D., Hosios, A. M., Muir, A., Chin, C. R., Freinkman, E., Jacks, T., Wolpin, B. M., Vitkup, D., & Vander Heiden, M. G. (2016). Tissue of origin dictates branched-chain amino acid metabolism in mutant Kras-driven cancers. *Science (New York, N.Y.)*, *353*(6304), 1161–1165. https://doi.org/10.1126/science.aaf5171

Chun, S. Y., Johnson, C., Washburn, J. G., Cruz-Correa, M. R., Dang, D. T., & Dang, L. H. (2010). Oncogenic KRAS modulates mitochondrial metabolism in human colon cancer cells by inducing HIF-1α and HIF-2α target genes. *Molecular cancer*, *9*, 293. https://doi.org/10.1186/1476-4598-9-293

Pickrell, A. M., & Youle, R. J. (2015). The roles of PINK1, parkin, and mitochondrial fidelity in Parkinson's disease. *Neuron*, *85*(2), 257–273. https://doi.org/10.1016/j.neuron.2014.12.007

Dorn, G. W., 2nd, Vega, R. B., & Kelly, D. P. (2015). Mitochondrial biogenesis and dynamics in the developing and diseased heart. *Genes & development*, *29*(19), 1981–1991. https://doi.org/10.1101/gad.269894.115

Quirós, P. M., Langer, T., & López-Otín, C. (2015). New roles for mitochondrial proteases in health, ageing and disease. *Nature reviews. Molecular cell biology*, *16*(6), 345–359. https://doi.org/10.1038/nrm3984

Correia-Melo, C., Marques, F. D., Anderson, R., Hewitt, G., Hewitt, R., Cole, J., Carroll, B. M., Miwa, S., Birch, J., Merz, A., Rushton, M. D., Charles, M., Jurk, D., Tait, S. W., Czapiewski, R., Greaves, L., Nelson, G., Bohlooly-Y, M., Rodriguez-Cuenca, S., Vidal-Puig, A., … Passos, J. F. (2016). Mitochondria are required for pro-ageing features of the senescent phenotype. *The EMBO journal*, *35*(7), 724–742. https://doi.org/10.15252/embj.201592862

Tait, S. W., Oberst, A., Quarato, G., Milasta, S., Haller, M., Wang, R., Karvela, M., Ichim, G., Yatim, N., Albert, M. L., Kidd, G., Wakefield, R., Frase, S., Krautwald, S., Linkermann, A., & Green, D. R. (2013). Widespread mitochondrial depletion via mitophagy does not compromise necroptosis. *Cell reports*, *5*(4), 878–885. https://doi.org/10.1016/j.celrep.2013.10.034

Soutar, M. P. M., Kempthorne, L., Annuario, E., Luft, C., Wray, S., Ketteler, R., Ludtmann, M. H. R., & Plun-Favreau, H. (2019). FBS/BSA media concentration determines CCCP's ability to depolarize mitochondria and activate PINK1-PRKN mitophagy. *Autophagy*, *15*(11), 2002–2011. https://doi.org/10.1080/15548627.2019.1603549

Ullah, M. F., Bhat, S. H., Hussain, E., Abu-Duhier, F., Ahmad, A., & Hadi, S. M. (2012). Ascorbic acid in cancer chemoprevention: translational perspectives and efficacy. *Current drug targets*, *13*(14), 1757–1771. https://doi.org/10.2174/138945012804545669

Cameron, E., & Pauling, L. (1976). Supplemental ascorbate in the supportive treatment of cancer: Prolongation of survival times in terminal human cancer. *Proceedings of the National Academy of Sciences of the United States of America*, *73*(10), 3685–3689. https://doi.org/10.1073/pnas.73.10.3685

Aguilera, O., Muñoz-Sagastibelza, M., Torrejón, B., Borrero-Palacios, A., Del Puerto-Nevado, L., Martínez-Useros, J., Rodriguez-Remirez, M., Zazo, S., García, E., Fraga, M., Rojo, F., & García-Foncillas, J. (2016). Vitamin C uncouples the Warburg metabolic switch in KRAS mutant colon cancer. *Oncotarget*, *7*(30), 47954–47965. https://doi.org/10.18632/oncotarget.10087

Aguilera, O., Muñoz-Sagastibelza, M., Torrejón, B., Borrero-Palacios, A., Del Puerto-Nevado, L., Martínez-Useros, J., Rodriguez-Remirez, M., Zazo, S., García, E., Fraga, M., Rojo, F., & García-Foncillas, J. (2016). Vitamin C uncouples the Warburg metabolic switch in KRAS mutant colon cancer. *Oncotarget*, *7*(30), 47954–47965. https://doi.org/10.18632/oncotarget.10087

Cenigaonandia-Campillo, A., Serna-Blasco, R., Gómez-Ocabo, L., Solanes-Casado, S., Baños-Herraiz, N., Puerto-Nevado, L. D., Cañas, J. A., Aceñero, M. J., García-Foncillas, J., & Aguilera, Ó. (2021). Vitamin C activates pyruvate dehydrogenase (PDH) targeting the mitochondrial tricarboxylic acid (TCA) cycle in hypoxic *KRAS* mutant colon cancer. *Theranostics*, *11*(8), 3595–3606. https://doi.org/10.7150/thno.51265

Wilkes, J. G., O'Leary, B. R., Du, J., Klinger, A. R., Sibenaller, Z. A., Doskey, C. M., Gibson-Corley, K. N., Alexander, M. S., Tsai, S., Buettner, G. R., & Cullen, J. J. (2018). Pharmacologic ascorbate ($P\text{-}AscH^-$) suppresses hypoxia-inducible Factor-1α (HIF-1α) in pancreatic adenocarcinoma. *Clinical & experimental metastasis*, *35*(1-2), 37–51. https://doi.org/10.1007/s10585-018-9876-z

Aronson S. M. (1994). Arsenic and old myths. *Rhode Island medicine*, *77*(7), 233–234.

Bak, D. W., Pizzagalli, M. D., & Weerapana, E. (2017). Identifying Functional Cysteine Residues in the Mitochondria. *ACS chemical biology*, *12*(4), 947–957. https://doi.org/10.1021/acschembio.6b01074

Wong, N., De Melo, J., & Tang, D. (2013). PKM2, a Central Point of Regulation in Cancer Metabolism. *International journal of cell biology*, *2013*, 242513. https://doi.org/10.1155/2013/242513

Zhang, H. N., Yang, L., Ling, J. Y., Czajkowsky, D. M., Wang, J. F., Zhang, X. W., Zhou, Y. M., Ge, F., Yang, M. K., Xiong, Q., Guo, S. J., Le, H. Y., Wu, S. F., Yan, W., Liu, B., Zhu, H., Chen, Z., & Tao, S. C. (2015). Systematic identification of arsenic-binding proteins reveals that hexokinase-2 is inhibited by arsenic. *Proceedings of the National Academy of Sciences of the United States of America*, *112*(49), 15084–15089. https://doi.org/10.1073/pnas.1521316112

An, H., Heo, J. S., Kim, P., Lian, Z., Lee, S., Park, J., Hong, E., Pang, K., Park, Y., Ooshima, A., Lee, J., Son, M., Park, H., Wu, Z., Park, K. S., Kim, S. J., Bae, I., & Yang, K. M. (2021). Tetraarsenic hexoxide enhances generation of mitochondrial ROS to promote pyroptosis by

inducing the activation of caspase-3/GSDME in triple-negative breast cancer cells. *Cell death & disease*, *12*(2), 159. https://doi.org/10.1038/s41419-021-03454-9

Akao, Y., Nakagawa, Y., & Akiyama, K. (1999). Arsenic trioxide induces apoptosis in neuroblastoma cell lines through the activation of caspase 3 in vitro. *FEBS letters*, *455*(1-2), 59–62. https://doi.org/10.1016/s0014-5793(99)00841-8

Eyvani, H., Moghaddaskho, F., Kabuli, M., Zekri, A., Momeny, M., Tavakkoly-Bazzaz, J., Alimoghaddam, K., Ghavamzadeh, A., & Ghaffari, S. H. (2016). Arsenic trioxide induces cell cycle arrest and alters DNA methylation patterns of cell cycle regulatory genes in colorectal cancer cells. *Life sciences*, *167*, 67–77. https://doi.org/10.1016/j.lfs.2016.10.020

Hayakawa, T., Kobayashi, Y., Cui, X., & Hirano, S. (2005). A new metabolic pathway of arsenite: arsenic-glutathione complexes are substrates for human arsenic methyltransferase Cyt19. *Archives of toxicology*, *79*(4), 183–191. https://doi.org/10.1007/s00204-004-0620-x

Palmeira, C. M., Teodoro, J. S., Amorim, J. A., Steegborn, C., Sinclair, D. A., & Rolo, A. P. (2019). Mitohormesis and metabolic health: The interplay between ROS, cAMP and sirtuins. *Free radical biology & medicine*, *141*, 483–491. https://doi.org/10.1016/j.freeradbiomed.2019.07.017

Wu, X., Park, M., Sarbassova, D. A., Ying, H., Lee, M. G., Bhattacharya, R., Ellis, L., Peterson, C. B., Hung, M. C., Lin, H. K., Bersimbaev, R. I., Song, M. S., & Sarbassov, D. D. (2020). A chirality-dependent action of vitamin C in suppressing Kirsten rat sarcoma mutant tumor growth by the oxidative combination: Rationale for cancer therapeutics. *International journal of cancer*, *146*(10), 2822–2828. https://doi.org/10.1002/ijc.32658

Baker, R. A., & Bruemmer, J. H. (1968). Oxidation of ascorbic acid by enzyme preparations from orange. *Fla State Hort Soc Proc*.

Siekevitz P (1957). "Powerhouse of the cell". *Scientific American*. **197** (1): 131–140. Bibcode:1957SciAm.197a.131S. doi:10.1038/scientificamerican0757-131

Zorov, D. B., Krasnikov, B. F., Kuzminova, A. E., Vysokikh MYu, & Zorova, L. D. (1997). Mitochondria revisited. Alternative functions of mitochondria. *Bioscience reports*, *17*(6), 507–520. https://doi.org/10.1023/a:1027304122259

Zong, W. X., Rabinowitz, J. D., & White, E. (2016). Mitochondria and Cancer. *Molecular cell*, *61*(5), 667–676. https://doi.org/10.1016/j.molcel.2016.02.011

Kochan, S. M. V., Malo, M. C., Jevtic, M., Jahn-Kelleter, H. M., Wani, G. A., Ndoci, K., Pérez-Revuelta, L., Gaedke, F., Schäffner, I., Lie, D. C., Schauss, A., & Bergami, M. (2024). Enhanced mitochondrial fusion during a critical period of synaptic plasticity in adult-born neurons. *Neuron*, S0896-6273(24)00167-3. Advance online publication. https://doi.org/10.1016/j.neuron.2024.03.013

Birky Jr, C. W. (1994). Relaxed and stringent genomes: why cytoplasmic genes don't obey Mendel's laws. *Journal of Heredity*, *85*(5), 355-365. https://doi.org/10.1093/oxfordjournals.jhered.a111480

Begimbetova, D., Burska, A. N., Baltabekova, A., Kussainova, A., Kukanova, A., Fazyl, F., Ibragimova, M., Manekenova, K., Makishev, A., Bersimbaev, R. I., & Sarbassov, D. D. (2024). The Vitamin C Enantiomers Possess a Comparable Potency in the Induction of Oxidative Stress in Cancer Cells but Differ in Their Toxicity. *International journal of molecular sciences*, *25*(5), 2531. https://doi.org/10.3390/ijms25052531